

Review

# Research Progress in Thermal Runaway Vent Gas Characteristics of Li-Ion Battery

**Mingming Qiu**  **Jianghong Liu**  **Beihua Cong**  **Yan Cui** <sup>1</sup> Ocean Science and Engineering College, Shanghai Maritime University, Shanghai 201306, China; 202130410107@stu.shmtu.edu.cn (M.Q.); 202030410162@stu.shmtu.edu.cn (Y.C.)<sup>2</sup> Shanghai Institute of Disaster Prevention and Relief, Tongji University, Shanghai 200092, China

\* Correspondence: liujh@shmtu.edu.cn (J.L.); bhcong@tongji.edu.cn (B.C.)

**Abstract:** The wide application of lithium-ion batteries (LIBs) brings along with it various safety problems, such as fire and explosion accidents. Aiming at the thermal runaway (TR) and fire problems of LIBs, we reviewed the evolution of TR within LIB and the release of TR gases and their hazards, as well as the research progress in recent years in the area of fire separation of LIBs. To begin with, physical, electrical, and thermal abuse are the three main factors leading to TR and the thermal stability of aging batteries significantly deteriorates. Furthermore, the decomposition of the electrolyte and the reaction between the active materials generates CO, CO<sub>2</sub>, H<sub>2</sub>, HF, and a variety of hydrocarbons. These TR gases have serious toxic and explosive hazards. In addition, fire separation can effectively delay the occurrence and propagation of TR within LIB modules. As a good heat-absorbing material, phase-change materials are widely used in the thermal management system and have a great prospect of wide applications in the fire separation of LIBs. Finally, the research on the TR gases' hazards of aging LIB and safer and more effective fire separation are prospected.

**Keywords:** Li-ion battery; thermal runaway; vent gas; explosion; toxicity; phase-change material

**Citation:** Qiu, M.; Liu, J.; Cong, B.; Cui, Y. Research Progress in Thermal Runaway Vent Gas Characteristics of Li-Ion Battery. *Batteries* **2023**, *9*, 411. <https://doi.org/10.3390/batteries9080411>

Academic Editor: Ivana Hasa

Received: 20 June 2023

Revised: 24 July 2023

Accepted: 2 August 2023

Published: 7 August 2023



**Copyright:** © 2023 by the authors. Licensee MDPI, Basel, Switzerland. This article is an open access article distributed under the terms and conditions of the Creative Commons Attribution (CC BY) license (<https://creativecommons.org/licenses/by/4.0/>).

## 1. Introduction

Due to their high energy density, being environmentally friendly, and long cycle life, LIBs have been widely used in mobile communications, transportation, new energy storage, and other fields. However, fire incidents caused by LIBs have become more and more frequent, with TR being a significant accident cause. TR is prone to occur during the mechanical, electrical, and thermal abuse of LIBs. The heat released by the internal short circuit of the battery and the chemical reaction between battery components are the primary heat sources that cause TR [1]. The LIBs in a TR state release a large amount of heat and gas. Some gases are toxic and explosive. As TR continues to intensify, with heat accumulation and gas bursts, it is easy to cause fire and explosion accidents in the batteries, causing severe damage to humans and the environment. Understanding the TR mechanism and gas-production behavior of LIBs is crucial for enhancing the internal material composition and safety management protocols of LIBs.

So far, some researchers have summarized and reviewed the research status of the TR of LIBs [2–5]. Huang et al. [2] provided a comprehensive overview of the causes, identification, and prevention of internal short circuits. Liao et al. [3] conducted a thorough examination of the potential causes and mechanisms of TR and various methods to monitor and detect its occurrence. Mallick et al. [4] delved into the origin and transmission of TR in LIBs. They also highlighted the significance of implementing multiple cooling techniques or preventive measures to avert fire risk. Tran et al. [5] discussed recent developments in approaches to LIB TR modeling, along with the prediction and detection of TR events. Zhang et al. [6] reviewed LIBs' thermal behavior, as well as TR modeling. The authors also delved into the underlying mechanisms of heat production, dispersion, and buildup within

the battery. Cui et al. [7] reached conclusions regarding the fire suppression mechanism and the effectiveness of water mist and analyzed a series of processes that further caused a fire after the TR of the battery, indicating that water mist is particularly well suited to contain and extinguish LIB fires.

Some researchers have reviewed the TR gas production of LIBs [8–10]. For example, Chen et al. [8] reviewed the flue-gas composition of LIB TR but did not discuss the harm of flue gas. Cui et al. [9] summarized the research status of TR gases in LIBs and only focused on the research progress of gas explosion hazards. Li et al. [10] discussed the research status in three aspects: gas-production mechanisms, gas analysis methods, and gas characteristics of TR gas of LIBs, without mentioning the influence of battery aging on TR gas of LIBs.

The existing review literature primarily uses common indexes, such as TR onset temperature and heat release rate, to summarize the characteristics and laws of TR, and lacks a summary of the effect of aging on the TR of LIBs. However, studies have shown that battery aging also causes TR and the TR characteristics of aging batteries differ from those of new batteries [11]. In order to comprehensively understand the characteristics and hazards of LIBs' TR vent gas, with aging batteries as the main research object, this paper provides a comprehensive assessment of the literature on current TR gas from two aspects. First, from the perspective of gas generation, the mechanism of TR gas generation is analyzed and the effects of different factors on gas generation are considered; second, in terms of the gas-generation hazards, the gas's toxicity and explosive hazards are examined. In addition, the recent research progress in LIB fire separations is also reviewed. Finally, the possible future direction of LIB's TR gas and fire separation is analyzed and prospected.

## 2. Li-Ion Battery Thermal Runaway

### 2.1. Li-Ion Battery Thermal Runaway Mechanism

With the wide application of LIBs, the safety problems it brings cannot be ignored, among which the TR problem is more prominent. TR is the phenomenon of uncontrollable rising battery temperature caused by the exothermic chain reaction of LIBs [12]. Generally, a LIB possesses a stable structure, allowing for the smooth exchange of  $\text{Li}^+$  between the anode and cathode during the charging and discharging process. However, the battery's inherent stability is vulnerable to various abusive influences, which may cause thermal hazards. As illustrated in Figure 1, the sources of such harm can be categorized into three main types, namely mechanical, electrical, and thermal factors. Manufacturing defects and battery aging can also result in TR [13].

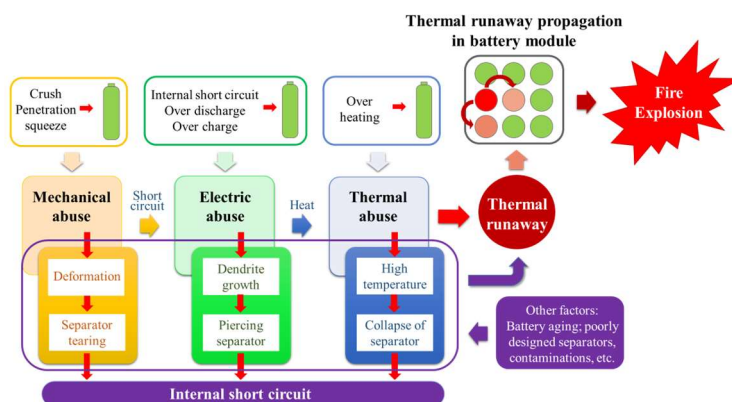


**Figure 1.** Diagram outlining the reasons for LIB fire incidents.

Mechanical abuse refers mainly to external forces, such as collision, acupuncture, and extrusion, when the battery is used, which cause destructive deformation. A mechanical failure in the separator or electrodes has the potential to initiate a short circuit, resulting in increased pressure, gas production, and an increase in temperature. In the most severe cases, TR can lead to ignition and, ultimately, to fire due to elevated temperature [14]. Jia et al. [15] conducted an extrusion test on the battery. As the extrusion speed increases, the

change rate of the battery voltage with the extrusion displacement also increases. In other words, the faster the impact speed on the battery, the greater the possibility of thermal safety accidents.

Electrical failure commonly involves external and internal short circuits, overcharging, and overdischarge. If the battery persists in charging beyond its upper charge limit, deposition of lithium metal may occur on the negative electrode surface [16]. At elevated temperatures, the presence of deposited lithium will elicit a reaction with the electrolyte, generating significant amounts of heat and gas [17]. The accumulation of such heat will result in a substantial spike in battery temperature, causing the destruction of the separator, decomposition of the electrode/electrolyte, and the initiation of other side reactions, resulting in serious TR. Wang et al. [18] analyzed the thermal diffusion path and high-temperature gas spillover path of overcharged lithium batteries. The heat produced by the exothermic reaction between the deposited lithium and electrolyte during the overcharge was found to be greater than 43%.

In addition to mechanical or electrical factors, thermal collapse can also be induced by external high temperatures and overheating. Excessive heat can cause the breakdown of the solid electrode interface (SEI) on the graphite surface and the depletion of the electrolyte in batteries. When the heat generated from internal reactions exceeds the dissipation, the internal temperature and pressure gradually increase, eventually leading to battery rupture and the emission of flammable gases. These gases can ignite spontaneously and cause a fire [19]. Clearly, battery TR stems from thermal abuse [13]. Peng et al. [20] simulated and analyzed the TR of batteries with various cathode materials. Their findings revealed that the cathode decomposition reaction played a significant role in the generation of heat within the batteries, with lithium manganate (LMO) exhibiting the highest initial decomposition temperature and most excellent stability. In particular, lithium iron phosphate (LFP) emerged as the safest cathode material because of its comparatively lower heat production rate compared to other materials, as illustrated in Figure 2. In addition, the excellent safety of LFP is also reflected in its good thermal stability, which is attributed to the stable olivine structure of LFP cathode material. The solid covalent bond in LFP enables it to maintain a highly stable crystal structure during charging and discharging, so it has higher safety performance and longer cycle life than LCO, LMO, and other cathode materials.

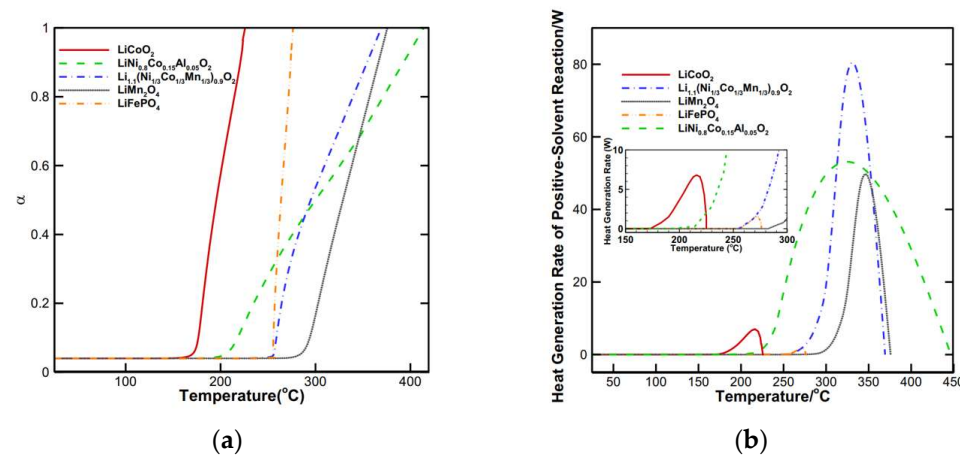


**Figure 2.** Comparison of the reaction degrees (a) and heat generation rates (b) of positive solvent for batteries of various cathode materials [20].

Apart from the above external factors, internal defects of the battery caused by poor manufacturing processes, such as poorly designed separators, material contaminations, and other manufacturing processes, can also cause battery breakdown and TR [21].

## 2.2. Aging Li-Ion Battery Thermal Runaway

LIBs are extensively used in various industries and the actual working environment is complex and changeable, which can easily cause different degrees of aging problems, such as increased internal resistance and capacity attenuation. It is widely recognized that the longevity of LIBs can be constrained by undesirable side reactions, such as the formation and rupture of SEI film, lithium precipitation, and so on. These reactions can impact various components of the cell, such as the electrolyte, active material, binder, conducting agents, current collectors, and separator, resulting in reduced capacity and/or increased overall cell impedance [22]. In addition, such side reactions may have a bearing on the safety of the cells. Capacity attenuation and increase in internal resistance are only the external manifestations of the aging of LIBs. The internal aging attenuation mechanism of LIBs mainly comprises two categories: the loss of electrode active material (LAM) and the loss of lithium inventory (LLI). This aging mechanism is visually depicted in Figure 3, as presented by Han et al. [23], through the use of a dual-tank model. This model compares the cathode and anode of the battery to two tanks and lithium ions to water. During charging, the movement of lithium ions from the cathode to the anode causes a decrease in the lithium density of the cathode and an increase in that of the anode, similar to the flow of water between two tanks. On the contrary, lithium ions move from the anode to the cathode during discharge. The fundamental aging mechanisms of LIBs are the LAM and LLI, which can be likened to changes in the tank and loss of water, respectively. In particular, the aging attenuation path of LIBs differs between cycle aging and calendar aging, leading to different external characteristics and safety performance.

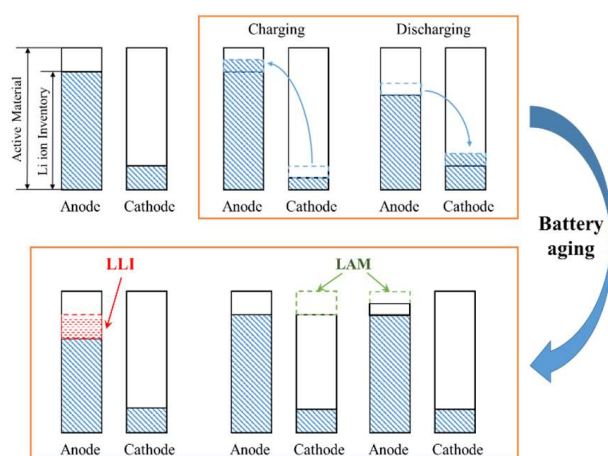


**Figure 3.** Dual-tank model.

In the battery-cycle test, the performance of new and old batteries is different. After the battery is aged at room temperature/high temperature, the battery's resistance to overcharge, short circuit, and other electrical abuse is reduced and the phenomenon of fire and explosion occurs during the experiment. In contrast, the new battery can withstand the above electrical abuse tests [24–26]. Some studies have shown that the thermal stability of the battery will deteriorate after the overcharge cycle, mainly reflected in the decrease in the initial temperature of the self-generated heat and the trigger, and the increase in maximum temperature [27]. Friesen et al. [28] tested the adiabatic TR of ternary LIBs after low-temperature cyclic aging at 0 °C. It was found that the initial temperature of the self-generated heat of the decaying battery was reduced from 90 °C to 30 °C. The rate of self-generated heat increased significantly in the temperature range of 30~100 °C and a new heat generation peak appeared, which was independent of SOC. In the research work of Zhang [29], it was also found that the battery was more likely to enter a TR state after aging. With the increase in the number of cycles, the TR behavior of the battery became more and more intense and the TR ejected more products. When the battery is cycled up to 300 times, the battery capacity decreases by about 10% (90% SOH) and the impedance

(series resistance) increases by about 10% [30]. The positive and negative electrodes of the battery after dissection were analyzed by SEM (scanning electron microscope) and XRD (X-ray diffractometer), respectively [26]. By comparing the LIB with 400 cycles and without cycles, it was found that there were lithium and lithium compounds on the surface of the anode after the cycle and the graphite structure partially collapsed. These phenomena have an adverse effect on the safety of LIBs. The solid electrolyte interface (SEI film) determines the thermal stability of the battery [31]. The thickness, morphology, and composition of the SEI affect the heat generated during the TR prebreakdown. Rapid charge and discharge of the battery during the cycle lead to rupture of the SEI film, which promotes the reaction between graphite and electrolyte, and then the thermal stability of the battery decreases [32].

The calendar aging process involves storing cells under specific conditions, commonly influenced by temperature and time. To obtain varying degrees of aging, cells were subjected to accelerated aging through storage at 55 °C and 100% SOC for durations ranging from 10 to 90 days. The samples were collected at intervals of 10, 20, 40, 68, and 90 days to obtain different aging states. Research shows that the self-heating temperature and TR temperature of the battery increase, while the exothermal rate during TR decreases [33]. This demonstrates that the thermal safety of the battery improved after calendar aging.

### 3. Li-Ion Battery Thermal Runaway Gas Production

#### 3.1. Gas-Production Mechanism and Composition and Content

The phenomenon of TR of LIBs is commonly characterized by the generation of substantial amounts of gas and heat. At elevated temperatures, the electrochemical processes within the battery are incredibly intricate, involving reactions such as the decomposition of the SEI film, the interactions between the electrode active material and the electrolyte, the decomposition of the electrolyte, and the reaction between the anode active material and the binder (see in Figure 4) [34,35].

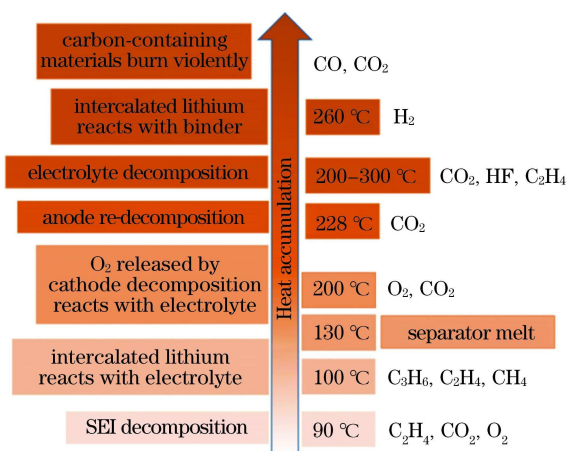


**Figure 4.** An overview of the TR process and gas generation of Li-ion battery [34].

Although these reactions do not occur sequentially or singularly, many occur simultaneously. The reactions are accompanied by a large amount of heat and gas generation. It has been tested that the production of TR gas of LIBs mainly contains CO, CO<sub>2</sub>, H<sub>2</sub>, CH<sub>4</sub>, C<sub>2</sub>H<sub>4</sub>, C<sub>3</sub>H<sub>6</sub>, C<sub>3</sub>H<sub>8</sub>, C<sub>4</sub>H<sub>10</sub>, C<sub>4</sub>H<sub>8</sub>, and other olefins and alkanes [36,37], of which CO, CO<sub>2</sub>, and H<sub>2</sub> generally account for more than 70% [8].

O<sub>2</sub> is an important intermediate product of CO and CO<sub>2</sub> gas generation and the decompositions of SEI membrane components and cathode materials are accompanied by the generation of O<sub>2</sub> [1]. O<sub>2</sub> reacts with the electrolyte to produce CO<sub>2</sub> when O<sub>2</sub> is sufficient. Otherwise, the reaction produces CO. In addition, some reactions during TR also generate CO and CO<sub>2</sub>, such as the decomposition of SEI membrane, complete or incomplete combustion of negative graphite, the reaction of CO with H<sub>2</sub>O at high temperatures, combustible gas combustion, etc. [9].

The reactions of lithium with the binder are the main ways to generate H<sub>2</sub>. Polyvinylidene fluoride (PVdF) and carboxymethyl cellulose (CMC) are the most commonly used binder materials. Defoliation of graphite particles occurs at or above 230 °C, where Li gets exposed to the electrolyte and the binder. Elevated temperatures of 260 °C or more may lead to a reaction between PVdF and Li, releasing H<sub>2</sub> in the process, as reported by Golubkov et al. [38]. Similarly, a comparable reaction between CMC and Li may occur beyond 250 °C.

Both the generation and decomposition of SEI film are accompanied by the generation of C<sub>2</sub>H<sub>4</sub> gas. When the temperature of TR of LIBs continues to rise, the reaction of Li on the anode surface with the organic solvent of the electrolyte generates more gaseous hydrocarbons, such as C<sub>3</sub>H<sub>6</sub>, C<sub>3</sub>H<sub>8</sub>, C<sub>4</sub>H<sub>10</sub>, etc. [10].

In addition to the above gases, phosphoryl fluoride (PFO<sub>3</sub>) and HF gases are also critical concerns in the TR gas production of LIBs. Based on an early assessment of battery composition, electrolyte salt (LiPF<sub>6</sub>) and the binder (PVdF) were found to be the primary sources of fluorine [39].

The experimentally measured release of the production of TR gas from LIBs can be as high as 0.27 mol, with a significant difference in the percentage of various gases [40]. In the case of a LiNi<sub>x</sub>Mn<sub>y</sub>Co<sub>z</sub>O<sub>2</sub> (NCM) power LIB with 20–80 Ah as an example, six gases, CO, CO<sub>2</sub>, H<sub>2</sub>, CH<sub>4</sub>, C<sub>2</sub>H<sub>4</sub>, and C<sub>3</sub>H<sub>6</sub>, account for about 99% of the total exhaust fraction, with CO<sub>2</sub> accounting for 36.56%, CO for 28.38%, H<sub>2</sub> for 22.27%, C<sub>2</sub>H<sub>4</sub> for 5.61%, CH<sub>4</sub> for 5.26%, C<sub>2</sub>H<sub>6</sub> for 0.99%, and C<sub>3</sub>H<sub>6</sub> for 0.52% [41].

### 3.2. Influencing Factors of Gas Production

The concentration of components and the amount of gas released by TR of LIBs are influenced by the SOC, electrode material, electrolyte, battery aging, and other factors.

#### 3.2.1. Electrode Material and Electrolyte

From the mechanism of TR gas production, it can be seen that the gas mainly comes from the reaction between the internal components of the battery. Therefore, the internal material composition of the battery affects the composition of TR gas. Under the same conditions (capacity or mass), the gas production of batteries with NiCoMn<sub>2</sub>O<sub>4</sub> and NiCoAl<sub>2</sub>O<sub>4</sub> systems is higher than that of LiFePO<sub>4</sub> batteries [38,42]. Golubkov et al. [38] conducted a comparative study on the TR gas-production characteristics of batteries with NCA and LFP as two different cathode materials. It was found that the gas production of the two batteries was quite different (see Figure 5). The gas released by the NCA battery was up to 317 mmol, while the gas released by the LFP battery was 61 mmol, and the NCA battery produced more CO and H<sub>2</sub> than the LFP battery. Huang et al. [42] found that the total amount of flammable gas released from the TR of NCM and LFP batteries was very different and the NCM module was much higher than that of the LFP module. The total combustible gases generated by the two were 21.09 g and 4.17 g, respectively. Combustible gases in LIBs were generated for a variety of reasons, including reactions between the electrolyte and lithium electrolyte, reactions between lithium and the binder, incomplete combustion of carbonate solvents, and reduction of carbon dioxide by lithium in the anode insert. Compared to the NCM battery, the LFP battery released a significantly lower amount of oxygen during cathode decomposition. This low amount of available oxygen limited the extent of electrolyte oxidation during TR, ultimately reducing the heat generated. This led to a noticeable difference in temperature between NCM LIB and LFP LIB during TR. The higher temperature of NCM LIB made its internal reaction more thorough and intense. Therefore, the combustible gas production in NCM LIB was higher than that in LFP LIB.

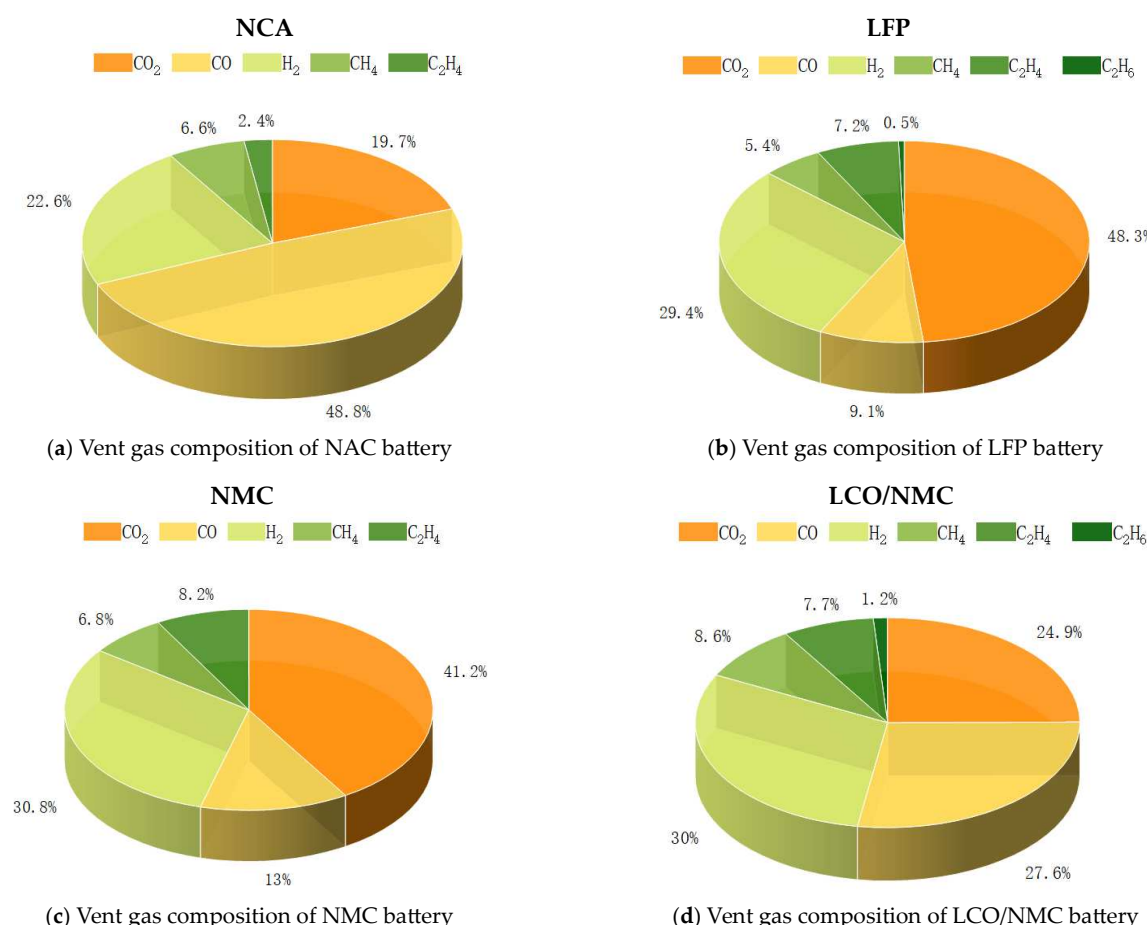


**Figure 5.** Vent gas component for 100% SOC battery TR.

### 3.2.2. The State of Charge

The concentration of the TR gas components and gas production are influenced by the SOC of the battery. The higher the SOC of the battery, the more gas is generated, and the gas components will change with the variation on the SOC. Somandepalli et al. [37] showed that the amount of TR gas released by the battery was proportional to the SOC. With the TR gas of the battery at 50%, 100%, and 150% SOC, the volume of the released gas was 0.8 L, 2.5 L, and 6.0 L, respectively. Usually, the higher the SOC of the battery, the higher the reactivity of the cathode and anode materials and the lower the thermal stability, which can easily trigger more internal chemical reactions. Therefore, the increase in SOC will result in a larger gas production under the same conditions. Koch et al. [41] came to a similar conclusion that the total amount of TR gas produced in the battery was closely related to the capacity of the battery, with an average of 1.96 L of gas occurring per Ah of capacity. Taking combustible gases CO and H<sub>2</sub> as examples, when the SOC value of the nickel-cobalt aluminate (NCA) battery was greater than 50%, the volume fraction of CO accounted for 40–50% of the total volume. For LFP batteries, H<sub>2</sub> was the most important combustible component and the volume fraction of H<sub>2</sub> also increased with the increase of the SOC value. When the SOC value was greater than 50%, the volume fraction of H<sub>2</sub> was about 20–30% of the total volume. There was no apparent correlation between other small molecules, including CH<sub>4</sub> and C<sub>2</sub>H<sub>4</sub>, and the battery SOC value. The sum of the two was less than 10% of the total gas volume [38].

### 3.2.3. Battery Aging

With the study of the factors that influence the TR gas production of LIBs, from the perspective of the mechanism of gas production, there is no doubt that the electrode

material and electrolyte of the battery itself will be considered. In terms of the process of gas production, the capacity of the battery becomes the preferred factor to be considered. In addition to this, the effect of the battery's circumstances during use on TR gas production should also be considered as an important research point.

After the battery is cyclically aged, its safety performance will be reduced to a certain extent. The main manifestations are the lower onset temperature and the earlier onset of TR of the battery [28,32]. Figure 6 depicts the relationship between the number of cycles and the TR onset time, temperature, and ignition time. In this study, 18650-type batteries with a positive electrode material of  $\text{LiNi}_{0.5}\text{Co}_{0.2}\text{Mn}_{0.3}\text{O}_2$  were used and five cycle numbers were selected to study the corresponding TR behavior. The data in Figure 6a show that TR occurs earlier and more easily as the cycle number increases. The decrease in battery safety is further illustrated by the phenomenon in the graph in Figure 6b, where the interval between gas release and ignition is 21 s for a cycle number of 0, and that time is reduced to only 1 s when the cycle number is increased to 60. The decrease of TR temperature and the advance of the TR gas release time further increase the gas production. Fleischhammer et al. [43] carried out battery aging experiments at 25 °C and found that the aged battery experienced an earlier jet valve time and more gas production during TR tests. Röder et al. [22] also conducted similar experiments. According to their experimental results, the reaction between the anode and the electrolyte of the battery after aging was advanced, resulting in increased gas production during the TR test.

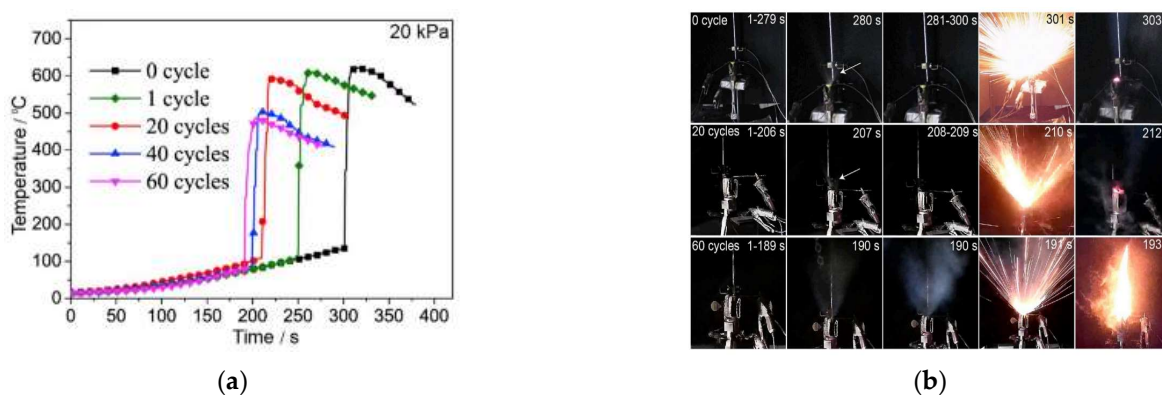


**Figure 6.** Surface temperature curves of the different cycles' batteries at 20 kPa (a) and the TR processes of different cycles' LIBs at 20 kPa (b) [32].

From the gas-production mechanism perspective, the decomposition reaction of SEI film, the reaction between electrolyte and electrode, and the decomposition reaction of the electrolyte itself are essential ways to generate TR gas. For the aging battery, in addition to the main reaction of  $\text{Li}^+$  insertion and extraction, more parasitic side reactions occur inside the battery during its working process; for example, the lithium precipitation reaction of the battery on the surface of the graphite anode, the formation and rupture reaction of the SEI film, etc. Furthermore, the lithium metal precipitated from the graphite anode is very active. It can react with the electrolyte at a lower temperature, resulting in a decrease in the initial temperature of self-generated heat and a sharp increase in the rate of self-generated heat, which is also an important reason for the decrease in the thermal stability of aging LIBs [11].

In the study of the TR gas production of LIBs, most of the batteries used in the experiments are new batteries and there is a certain lack of research related to the TR gas production of aging batteries. LIBs currently in use have different degrees of aging, and the performance of the battery after aging occurs is different from that of a new battery for most of its life cycle [44]. The effect of aging on TR gas production in LIBs, and the mechanism of it, should be further investigated.

### 3.3. Hazard Characteristics of Gas Production

The gas produced by the TR of LIBs contains toxic and flammable gases, which can harm the safety of people's lives and properties. Therefore, the toxicity and explosive hazards of the gas produced by the TR of LIBs are the key concerns of current researchers.

#### 3.3.1. Gas Toxicity Hazards

It is found that the common toxic gases detected in the TR release gas of LIBs are CO, HF, SO<sub>2</sub>, POF<sub>3</sub>, organic compounds, and so on. The types of toxic gases produced are closely related to battery materials, such as electrode materials, electrolytes, solvents, additives, flexible packaging, and the SOC of the battery [45].

The widely used LiPF<sub>6</sub> and binder PVdF in the battery electrolyte make the presence of HF and fluoride gas inevitable in the TR gas. At high temperatures, fluorine in the electrolyte and PVdF can produce gaseous byproducts such as hydrogen fluoride HF, phosphorus pentafluoride (PF<sub>5</sub>), and POF<sub>3</sub> to a limited degree. In the fire tests, HF gas was detected in all tests, whether a soft pack battery, a cylindrical battery, or a laptop battery pack, but the amount of gas produced differed [46]. For every 1 g of weight reduction in the battery, 16 mg, 15 mg, and 7.3 mg of HF gas were produced by the soft pack, cylindrical, and Lenovo laptop battery packs, respectively. In addition, phosphorus fluoride gas can be detected in the TR gas production of the LiCoO<sub>2</sub> (LCO) cell at 0% SOC, which acts as an intermediate compound in the chemical reaction [47]. POF<sub>3</sub> has been identified as a reactive intermediate [48] that will undergo reactions with various organic substances or water, leading to the eventual production of HF.

The effect of SOC on the toxicity of TR gases is reflected in the fact that the concentration and yield of each toxic gas vary with SOC. For CO, the production of CO increases as the SOC increases. That is because, the more energy stored in the cell, the more conducive to incomplete combustion [49]. Interestingly, the trend observed in total HF gas differs from the expected trend observed in CO versus SOC and previous researchers [39,46] have followed a similar opposite trend (increased HF with decreased SOC).

In addition to the internal cell materials mentioned above, externally applied water spray also affects the toxic gas. According to research by Yuan et al. [50], using water as an agent resulted in higher maximum concentrations of toxic gas emissions, including HF, CO, and H<sub>2</sub>. The primary source of HF is the thermal decomposition of LiPF<sub>6</sub> and electrolyte solvents, which occurs at higher temperatures. The addition of water triggers a reaction with PF<sub>5</sub>, subsequently initiating carbonate electrolyte decomposition based on LiPF<sub>6</sub>. The outcome of this process is a significant increase in the production of HF, as illustrated in Figure 7 [51]. Despite increasing the rate of HF production, it is worth noting that the overall production of HF is not altered [47]. It is also essential to recognize that water mists with surfactants positively reduce the potential for explosions of TR gas [50]. There are two distinct mechanisms by which water mist effectively suppresses explosions. Firstly, it provides a cooling effect on flames, effectively preventing heat transfer to unburned gas. Second, the mist dilutes the concentrations of combustible gases, such as CO, rendering them less reactive. That leads to weakening gas-reaction and transmission rates, culminating in preventing any chain reactions that may lead to an explosion [7].

According to statistics from the International Association of Fire and Rescue Services (CTIF) on related fire accidents, toxic smoke from fires is the main culprit of fire-related deaths and injuries. Smoke from LIB fires has been shown to contain a large amount of poisonous gases, so it is necessary to analyze and evaluate the toxicity of these gases quantitatively. According to the different mechanisms of action of various gases on the human body, toxic gases can be divided into asphyxiating and irritating. Therefore, the fractional effective dose (FED) method for asphyxiating gases and the fractional effective concentration (FEC) method for irritating gases are commonly used to evaluate the toxic hazards of toxic gases quantitatively. The effects of asphyxiating gases (CO, CO<sub>2</sub>) have a cumulative effect. Their hazards are not only related to the gas concentration but also to the exposure time of escapees. The principle of FED is shown in Equations (1) and (2) [52];

the effects of irritant gases (HF, HBr, HCl, SO<sub>2</sub>, NO<sub>2</sub>, Acrolein, Formaldehyde, etc.) are immediate and only related to the gas concentration. There are diverse irritant gases and their combined toxic effects can be calculated by Equation (3). In this evaluation method, a FED or FEC value equal to one means that 50% of the people in this fire scenario will lose the ability to escape [53].

$$\text{FED} = \sum_{t_1}^{t_2} \frac{V_{\text{CO}_2} \varphi_{\text{CO}}}{35000} \Delta t + \sum_{t_1}^{t_2} \frac{(V_{\text{CO}_2} \varphi_{\text{HCN}})^{2.36}}{1.2 \times 10^6} \Delta t \quad (1)$$

$$V_{\text{CO}_2} = \frac{\exp([CO_2])}{5} \quad (2)$$

where  $\varphi$  is the concentration of each gas in  $\mu\text{L/L}$ ,  $[CO_2]$  is the volume fraction of CO<sub>2</sub>, and  $\Delta t$  is the time increment.

$$\text{FEC} = \frac{[\text{HCl}]}{\text{IC}_{\text{HCl}}} + \frac{[\text{HBr}]}{\text{IC}_{\text{HBr}}} + \frac{[\text{HF}]}{\text{IC}_{\text{HF}}} + \frac{[\text{SO}_2]}{\text{IC}_{\text{SO}_2}} + \frac{[\text{NO}_2]}{\text{IC}_{\text{NO}_2}} + \frac{[\text{CH}_2 = \text{CH} - \text{CHO}]}{\text{IC}_{\text{CH}_2=\text{CH}-\text{CHO}}} + \frac{[\text{HCHO}]}{\text{IC}_{\text{HCHO}}} + \sum \frac{[\text{Irritant gases}]}{\text{IC}_i} \quad (3)$$

Concentrations in the formula are expressed in  $10^{-6}$ .

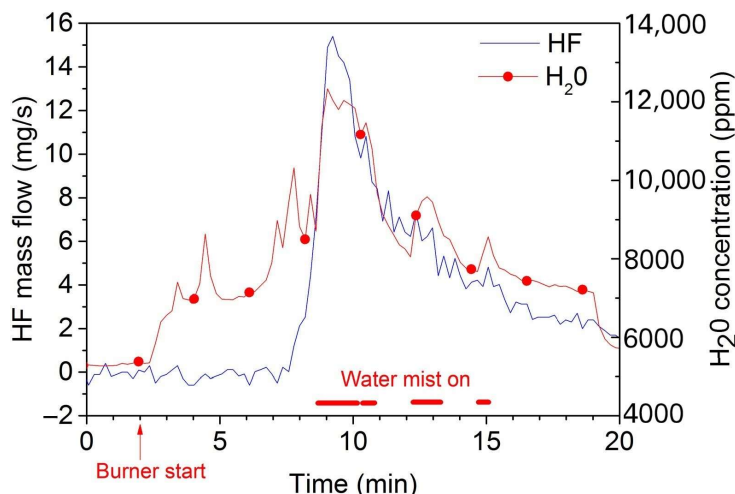


**Figure 7.** HF mass flow and water concentration [46].

The two models mentioned above in the present studies are often used to evaluate the toxicity of gases released from LIB TR. When the severity of gas toxicity is calculated, the gas is divided into two types of irritation and asphyxiation for independent consideration, making the calculation results more effective. Based on the validity of the above models, Zhang et al. [54] combined the FED equation with the ignition parameter (Equation (4)) to establish a kinetic model of the TR gas toxicity of the battery to characterize the consequences caused by gas toxicity.

$$V = SP = \frac{1}{TI} \times \frac{L_{\text{FED}}}{t_{X\text{FED}=1}} \quad (4)$$

where V is the risk rate, S is the probability of TR of the battery, P is the toxicity hazard, and  $t_{X\text{FED}=1}$  is the time elapsed from the start of TR to an  $X_{\text{FED}}$  value of 1.

The types and concentrations of toxic gases in TR gases are influenced by factors such as SOC and cell internal materials, and there is no doubt that the degree of toxicity of these gases will vary with these factors. The FED and FEC values of the gases will increase with the increase of SOC for both large-size power cells and small-size cells. Peng et al. [55] conducted a systematic study of thermal and gaseous toxicity hazards of large-size power-cell fires by experimental platform and FTIR. It was found that both FED and FEC values increased with increasing SOC. Under well-ventilated conditions, the FEC value from

single-cell combustion was as high as 0.8. This result was similar to the findings of Lecocq et al. [49]. High SOC cells are at increased risk of toxicity from releasing TR gases. When comparing the hazards of asphyxiating and irritant gases, the irritant gas dominates the total gas toxicity level and HF contributes the most prominently. In addition to the two evaluation models, FED and FEC, Ribière et al. [39] evaluated the toxicity hazard of each gas using the French industrial standards, namely the irreversible effect threshold (IET) and the first lethal effect threshold (FLET), for the main gas products HF, CO, NO, SO<sub>2</sub>, and HCl. The results also showed that HF gas has the most significant toxicity hazard.

In addition, the toxicity of gases changes accordingly after the battery has been cyclically aged. Aging battery TR is stronger and releases less heat, resulting in low combustion efficiency, and, then, generates more toxic gases. Based on the FED model, analyzing the final TR gas toxicity with different aging degrees [29], it was found that the cumulative effect of asphyxiating gases in aging batteries was higher than that in fresh batteries and more quickly reached the catastrophic concentration.

From the above analysis, it is clear that fluorine-based molecules are vital points in the field of battery safety. At the same time, it is also challenging to study how to reduce the toxic hazards of TR gas in LIBs. Nowadays, LiPF<sub>6</sub> and PVdF are widely used in the production of LIBs. How to find a balance between meeting demand and reducing the harm they cause is a challenging issue.

The disadvantage of using IET and FLET values to evaluate LIB TR gas compared to the FED and FEC models is that the time factor is not considered. Comparatively, the FED and FEC models provide more comprehensive results. However, it also has shortcomings. Both models have some assumptions, such as no reaction between toxic gases, which limits the application of these models. Future studies should further refine and improve them. The LIB TR gas compositions are complex and influenced by multiple factors. Therefore, an evaluation model should be able to consider all gases comprehensively and reflect their toxic contribution values. With the change of time and space, the toxic hazards of the gases will keep changing under certain circumstances. For example, in a confined space, the longer the time, the greater the accumulation of gases. And, in an open external environment, there are wind and obstructions. Thus, when evaluating the battery TR gas toxicity hazard, it also needs to be discussed in terms of classification depending on the scenario.

### 3.3.2. Gas Explosive Hazards

In the recent study conducted by Cui et al. [56] on a full-scale battery electric vehicle (BEV), a substantial white smoke emanated from the EV's battery pack (as depicted in Figure 8a). The smoke was released intermittently and it took only 7 s to induce a severe explosion. The fixed structure of the hood of the automobile was damaged by the shock wave (Figure 8b). This explosion phenomenon was similar to that observed in the previous experiment [57]. The white smoke comprised electrolyte vapors, C<sub>x</sub>H<sub>y</sub>, CO, and H<sub>2</sub> emitted from the TR batteries. Lamb et al. [58] measured the amounts and species of gas produced during the thermal decomposition of the common electrolyte components ethylene carbonate (EC), diethyl carbonate (DEC), dimethyl carbonate (DMC), and ethyl methyl carbonate (EMC). All tests showed the production of flammable gases in quantities sufficient to render the resulting mixture flammable in air. Therefore, among the gases released from the TR of LIBs, in addition to toxic gases, the hazard of explosive gases is also one of the key concerns. The current study usually uses the explosion limit, explosion overpressure, and laminar flow flame speed as three indicators to describe the battery TR gas ignition and explosion hazards.



**Figure 8.** The smoke released from BEV A (a) and explosion during the test (b) [56].

There are three methods to study the explosion limit of TR gas in LIBs: the formula calculation method, the experimental measurement method, and the simulation method. Scholars currently use the formula calculation method and the practical measurement method more. According to the literature, three ways are commonly used to calculate the explosion limit [59]. The first is for calculating the explosion limit of a single combustible gas, often referred to as the empirical formula method. The second is used to calculate the explosion limit of multiple flammable gas mixtures, known as the Le-Chatelier formula method (L-C formula), see Equation (5). Third is to calculate the explosive limit of the combustible gas mixture containing inert gases. When there is an inert gas in the mix, the explosion limit of the mixture can still be calculated using the L-C formula. But it requires the combination of an inert gas and a combustible gas in one group, after which the group of recombinant gases is used as a new flammable gas. The volume fraction of the recombinant gas in the mixture is the sum of the volume fraction of the inert gas and the flammable gas. The explosion limit of the recombinant gas needs to be redetermined. First, calculate the volume ratio of inert gas to combustible gas in the group of gases. Then, find out the explosion limit of the group of gases in Figure 9. Finally, substitute it into the L-C formula for calculation. LIB TR gas composition is complex, containing a variety of combustible and inert gases, often using the third calculation method to determine the explosive limit of the gas.

$$(LEL)_{mix} = \left[ \sum_{i=1}^n \frac{X_i}{(LFL)_i} \right]^{-1} \times 100 \quad (5)$$

where  $(LEL)_{mix}$  is the explosion-limit value of the mixture;  $(LFL)_i$  is the explosion-limit value of component  $i$ ;  $X_i$  is the volume fraction of component  $i$ .

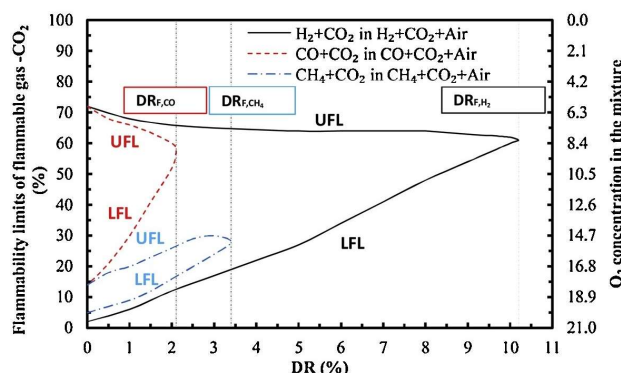


**Figure 9.** Flammability limits of flammable gas–CO<sub>2</sub> in air [60].

Guo et al. [61] used the above mathematical model to calculate the TR explosion limit of LIB. The lower explosion limit (LEL) was 6.22% and the upper explosion limit (UEL) was 38.4% of LIB at 100% SOC. In fact, the explosion limit of LIB TR gas is not a fixed value. SOC and electrode material of the battery are important influencing factors and, of course, different experimental conditions and methods will lead to different results. The LEL values are less sensitive to changes in the battery SOC. On the contrary, the UEL of the gas is more affected by the SOC and it usually becomes larger as the SOC increases. It can be concluded that the explosion-limit range of the gas expands with the increase of SOC. Li et al. [60] used the L-C model to calculate the explosion-limit values of TR gas at different SOCs for NCA and LFP cells and the calculated curve between the explosion limit and the SOC formed a peninsula (see Figure 10). The trend of the explosion-limit range in the figure is roughly the same as that of the above findings. It also can be found that the explosion range of different types of batteries is also different. In particular, when the battery SOC is at 25%, the explosion range of an NCA battery is about twice as large as that of an LFP battery. But both achieve the maximum at 100% SOC.

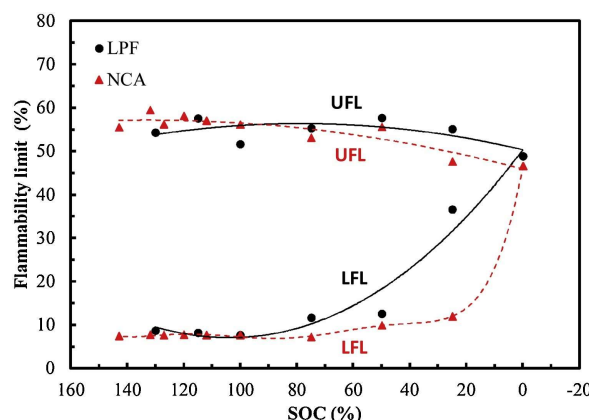


**Figure 10.** Comparison of flammability limits of flammable gases emitted from LFP and NCA [60].

Based on the results of Zhang et al. [62], the LEL follows the same trend as the alkane content, while the UEL shares a similar trend with the unsaturated hydrocarbon content. Compared to saturated hydrocarbons, the stability of the double bond structure of unsaturated hydrocarbons is worse and its reaction activation energy is higher. When the content of unsaturated hydrocarbons in TR gas increases significantly, the gas explosion-limit range will increase.

In terms of experimental studies, Karp [63] used a constant volume incendiary bomb device to test the explosive limit of thermally uncontrolled gases and judged flammability based on a pressure rise rate greater than or equal to 5% within the incendiary bomb after ignition. Compared with the experimental results and calculated outcomes through the L-C formula, the differences are less than 5%, indicating that the L-C formula can accurately calculate the TR gas explosion limit. Chen et al. [64] conducted a test on the TR gas LEL using the FRTA explosion-limit apparatus. The test results were also compared with those calculated by Equation (5), with a maximum error of 2.1%. In fact, the theoretical calculation formula ignores the effects of binding energy, incomplete combustion, and decomposition of burn products. Errors may also arise due to the influence of instrumentation. However, the experimentally measured gas explosion limit is relatively more reflective of the real situation of thermally uncontrolled gases.

Simulation is also helpful in determining the gas explosion limit and evaluating the explosive hazard. Notably, Ma et al. [65] conducted a comprehensive numerical investigation on the explosion limit of TR gas derived from NCA batteries using the CHEMKIN 2.0 code. This numerical analysis revealed that the UEL exponentially increases with rising SOC and peaks at 62% SOC. As SOC continues to grow, the UEL subsequently drops. Conversely, the LEL remains relatively constant when SOC is greater than 75%. Finally, LEL

reaches its minimum at 75% or 100% SOC. Baird et al. [66] used the open-source program Cantera to calculate the explosion limit, the laminar flame propagation velocity, and the maximum overpressure of the TR gas to comprehensively assess the explosion hazard. TR gas from NCA and LCO batteries produced a higher flame velocity and maximum overpressure, while LFP batteries had a lower flammable limit. Simulations can be used to accurately calculate the explosion limits of TR gas production at different initial conditions with detailed chemical-reaction kinetics, which is more tractable and compensates for the shortcomings of equation calculations and experimental measurements [65]. In addition, the explosion simulation software FLACS has commonly been used in simulating gas explosions. Regarding LIB explosion, it is mainly used to simulate the explosion of energy-storage plants [67]. In future studies, FLACS can be considered for the explosion simulation of small LIB modules.

In addition to the explosion limit, explosion overpressure, and laminar flame velocity, the explosive hazard of TR gases in LIBs can be assessed by combining minimum ignition energy, temperature, TR time, explosion-power index, and total explosion energy. Kan et al. [68] formulated a specific type of LIB TR gas according to its components and concentration and measured the minimum ignition energy of the gas to be 0.3 MJ, which is closer to the minimum ignition energy of acetylene, propane, and other gases. Studying the explosive hazards of LIB TR gas is vital to improving LIB's safety in the application. In future research, the explosive hazards of LIB TR gas can be considered from more perspectives and the explosion hazard evaluation model should be more comprehensive and practical.

#### 4. Fire Separation

As mentioned in the previous sections, LIB TR releases many gases. In some specific scenarios, the toxicity threat and explosion hazard of the gases greatly exacerbate the consequences of TR accidents. In addition to the gases, the large amount of heat released during the TR process is also a threat that cannot be ignored. The accumulation of heat leads to a rise in battery temperature, which, in turn, triggers more exothermic reactions, further increasing the release of heat and causing TR to become more and more severe. LIBs are always present in the form of battery modules in numerous applications. It is well known that LIB TR is propagating. When a TR occurs in one of the cells of the battery module, it is likely to trigger TRs in neighboring cells, or even in more distant cells, due to heat transmission. Cui et al. [69] found in their experiments that, when the first cell in a LIB module experienced an overheating TR, it caused the TR of the cells in the module to propagate discretely, as shown in Figure 11. The consequences of a single cell's TR could be catastrophic when the TR is completely propagated to the whole battery pack. As LIBs are widely used in electric vehicles, fire, and explosion accidents due to battery TR become more frequent. According to incomplete statistics, between 2019 and 2020, 223 combustion events occurred in multiple types of electric vehicles across the country [70]. It can be seen that, for the safe use of LIBs, it is crucial to keep the batteries at a suitable operating temperature and, if necessary, take effective heat dissipation and insulation measures to prevent the propagation of TR and other means of protection. Common protective measures include battery thermal management systems and fire-separation measures. A thermal management system aims to improve the thermal performance of the battery and control the operating temperature and temperature difference of the battery system under normal operating conditions. Fire separation is a means of protection to inhibit the propagation of TR batteries within the module to the surrounding batteries. The inhibition method is divided into two aspects. On the one hand, heat insulation materials can be added between the batteries to prevent the heat of the runaway battery from spreading to the surrounding area and to isolate the combustible ejecta and flames. On the other hand, materials capable of absorbing heat can be used to prevent heat from accumulating and to improve the heat-dissipation performance.

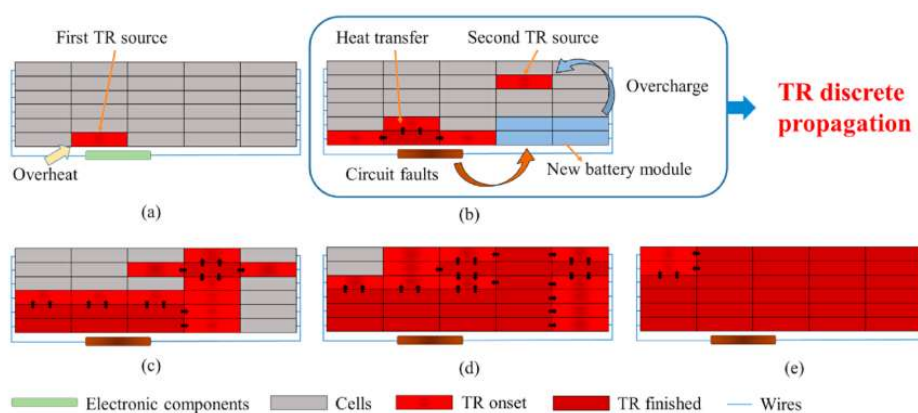


**Figure 11.** Schematic of the discrete propagation of TR in a battery module [69].

#### 4.1. Insulation Technology

TR propagation within a battery pack usually results from multiple forms of heat transmission, such as heat conduction, heat radiation, and heat convection, from the cell that first experiences TR to the other cells. It can be seen that establishing a thermal barrier between batteries to prevent TR batteries from transferring heat to other batteries is an effective means to inhibit TR propagation and avoid fire and explosion accidents in LIBs [71].

In order to achieve thermal transmission between batteries, the method of filling heat-insulating and flame-retardant materials between batteries is usually adopted. Berdichevsky et al. [72] inserted adiabatic flame-retardant plates and radiation-reflecting metal plates between the battery layers, blocking the heat propagation during TR by reducing the heat conduction and radiation between different battery layers. Mehta et al. [73] designed a thermal barrier using expansion materials, effectively preventing the heat from spreading. Lopez et al. [74] placed insulating materials, radiation barriers, and refractory expansion blocks between the cells. Chen et al. [75] sandwiched epoxy-resin plates between square aluminum shell batteries. The result showed that the epoxy-resin plates reduced the maximum temperature of the battery module and prolonged the propagation time of TR between adjacent batteries. Qin et al. [76], on the other hand, used fiberglass to separate cylindrical batteries. Fiberglass panels can significantly improve the safety of LIBs.

With good thermal insulation performance and low dosage, aerogel is widely used to inhibit the spread of TR in battery modules [77]. When TR occurs in the cell in the LIB module, the aerogel heat insulation sheet can play the key role of heat insulation, delaying or blocking the accident. In case of overheating and combustion, the nanopore structure of  $\text{SiO}_2$ , which is the main component of the aerogel heat insulator, can effectively block or delay the spread of fire, providing enough time for escape [78]. Hu et al. [79] placed a 1-mm-thick aerogel between batteries and found that the presence of aerogel thermal insulation blocked the effect of TR ejecta on other monomers and weakened thermal radiation and thermal convection effects. Shen et al. [80] investigated the barrier effect of aerogel on the TR of battery packs and compared the barrier effect of different thicknesses of thermal insulation interlayers. The TR propagation was effectively blocked when a 6-mm-thick aerogel thermal insulation sandwich was used.

Adding insulation materials with low thermal conductivity between batteries can block heat transfer between batteries. Still, it relatively reduces the heat-dissipation conditions of the batteries, which can easily lead to the accumulation of heat.

#### 4.2. Phase-Change Material

Considering the drawbacks of thermal insulation, there is a need to reduce the heat accumulation in the battery and improve the heat-dissipation ability of the battery. Due to their excellent ability to absorb heat, phase-change materials (PCM) have been widely studied and applied in the thermal management and fire separation of LIBs. According to

the molecular structure, PCM can be categorized into inorganic materials (e.g., hydrated salts) and organic materials (e.g., paraffin) [81].

Due to its low corrosiveness and cost, organic PCM is the most widely used PCM in electrical systems. Wike et al. [82] used a 18650 LIB pack as a research object, filled the battery-pack gap with PCM, and triggered one of the cells to undergo TR. It was found that the presence of PCM can effectively inhibit the thermal impact of the triggered battery on the surrounding batteries. When the cell temperature reaches the melting point of the PCM, the material melts and absorbs heat as a way to prevent TR propagation.

However, PCM has a critical drawback; it is flammable, especially paraffin-based organic PCM. The latent heat of the phase transition is limited. Although it can do well to inhibit the cyclic heat generation of the battery, it is not easy to fully absorb the heat released during the TR. Zhi et al. [83] investigated the effect of PCM on the propagation of TR. They found that the battery module with PCM rather enhances the heat transfer and the risk of ignition of the failing cell. To solve these problems, people try to combine PCM with other flame retardant/insulation materials to design safer thermal protection materials. Weng et al. [84] developed and studied composite PCM (CPCM) containing flame-retardant additives. The cooling performance of CPCM was reduced when a larger mass fraction of flame-retardant additives was added but it positively delayed the cell fire time and reduced the heat release rate. Dai et al. [85] added hydroxide flame retardant to organic PCM to minimize the fire hazard. Talele et al. [86] applied ceramic-coated heat-resistant liners to the walls of PCM to delay the TR triggering time. Weng et al. [87] investigated the heat dissipation and insulation ability of the combination of PCM and aerogel felt (see Figure 12). The results show that PCM can play a significant role in quenching the flame but it will lead to the acceleration of the TR propagation process, while the addition of aerogel can effectively retard the TR propagation. When facing modules with large-size cells, the coupling of aerogel and PCM can also effectively inhibit TR propagation and improve the heat-dissipation conditions [88].

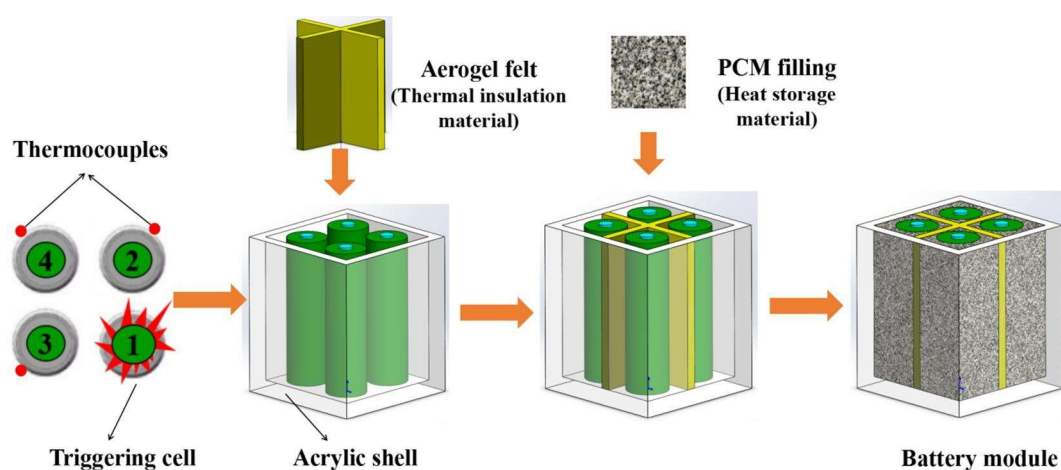


**Figure 12.** Using aerogel felt coupled with PCM for fire separation of the battery module [87].

Inorganic PCM (IPCM) is corrosive and has defects such as supercooling, dehydration, leakage, and phase separation during the phase-change process, which restricts its application in batteries. However, compared with organic PCM, inorganic PCM features nonflammability and high latent heat of phase change. Given these advantages, Galazutdinova et al. [89] added IPCM (mixture of  $MgCl_2 \cdot 6H_2O$  and  $Mg(NO_3)_2 \cdot 6H_2O$ ) for the first time, to LIBs and tested it in TR tests, which confirmed the effectiveness of the IPCM in preventing the propagation of TR. Subsequently, Cao et al. [90] investigated and designed a composite IPCM by doping IPCM (sodium acetate trihydrate, SAT) into expanded graphite (EG). Numerical TR-simulation experiments using the numerical thermochemical heat-storage (TCHS) model were performed and the results showed that SAT/EG could completely suppress TR propagation (see Figure 13). In order to solve the above defects of

IPCM, in the study of Ping et al. [81], nanoencapsulation of IPCM (EIPCM) was proposed to avoid the problems of leakage and water evaporation during the phase-change process. It was found in the experiments that the EIPCM has good thermal management effects and TR-suppression performance (see Figure 14).

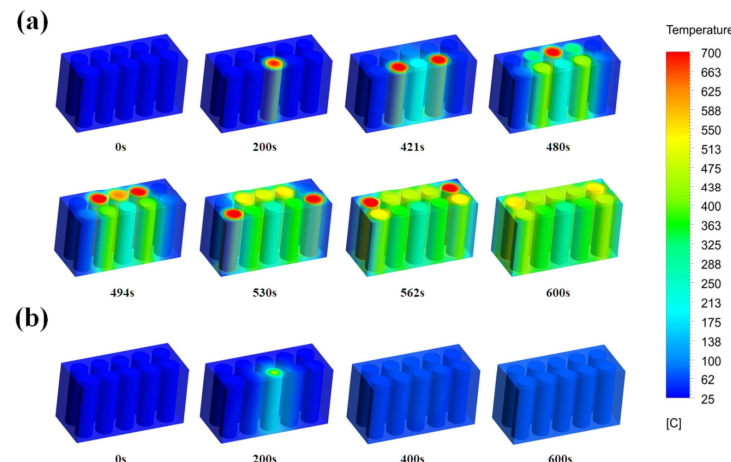


**Figure 13.** Comparison of the results of TR propagation simulated by the TCHS model: with polyvinyl chloride (a) and SAT/EG (b) [90].

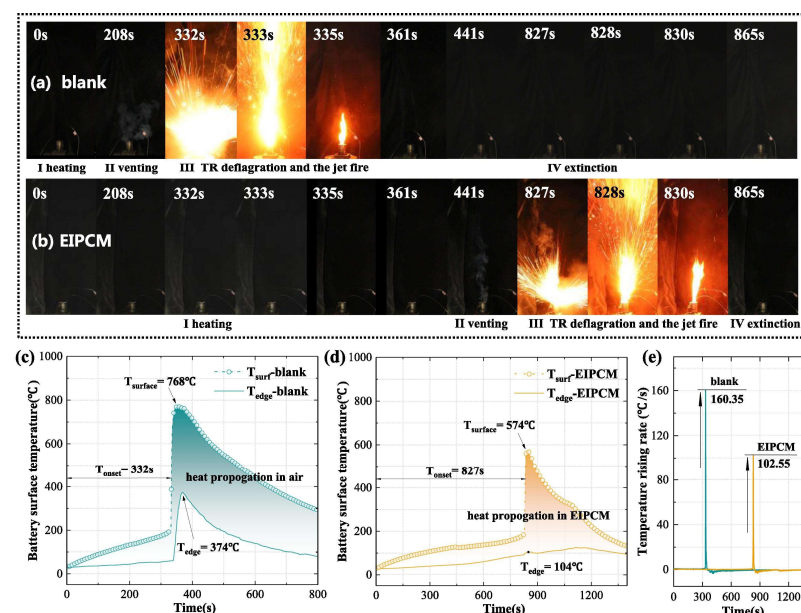


**Figure 14.** (a,b) TR process and (c,d,e) temperature changes of cells with and without EIPCM [81].

In summary, it can be seen that PCM has a good development prospect in thermal management and fire separation of batteries. Although using organic PCM as a fire-separation material increases the fire hazard of battery packs, the safety and thermal insulation performance of organic PCM can be improved by coupling it with thermal insulation materials such as aerogel. The shortcomings of IPCM severely limit its wide application in electrical systems. However, its incombustibility, high heat-storage density, and low cost are fully compatible with the requirements for battery fire-separation materials. Several studies have also verified their feasibility for inhibiting the propagation of battery TR. That shows that IPCMs have a great prospect of wide application. Future research should address these shortcomings, improve the performance of IPCM, and develop a safer and more efficient fire-separation material.

## 5. Conclusions and Outlook

The safety issue brought by LIB TR has become a key problem to be solved in its wide application. Numerous scholars have conducted in-depth and comprehensive research on this issue. In this paper, the toxic and explosive hazards of TR gases and the fire separation of batteries are reviewed.

Mechanical, electrical, and thermal abuse are the three main factors leading to TR in LIBs. Irreversible exothermic reactions occur inside the battery during abuse. The internal short circuit and the reaction between electrolyte and electrodes are the primary heat sources. When TR occurs in aging batteries, their thermal stability decreases significantly. It is mainly manifested in decreasing initial temperature, advancing beginning time, and increasing gas production of TR. The chain reaction of the TR process generates a large amount of gases, mainly including CO, CO<sub>2</sub>, H<sub>2</sub>, CH<sub>4</sub>, C<sub>2</sub>H<sub>4</sub>, C<sub>3</sub>H<sub>6</sub>, etc. Various aspects, such as SOC, electrode materials, electrolytes, battery aging, and other factors, affect the concentration of the gas components, release amount, and other characteristics.

The TR gases include a range of hazardous and potentially explosive gases that have raised concerns among researchers. The FED and FEC models are effective methods used to evaluate the toxicity hazard of LIB TR gases quantitatively. They can estimate the hazards of the asphyxiating effects of CO and HCN, and the irritating impact of HF and SO<sub>2</sub> on escapees. It was found that HF is the most toxic hazard among TR gases. Fluorine is derived from LiPF<sub>6</sub> and PVdF binders, widely used in battery electrolytes. In the future, safer and more environmentally friendly lithium salts and binders are yet to be developed and researched. TR gases contain a large amount of flammable gases, which pose severe fire and explosion hazards. After experimental measurements and formula calculations, the explosion-limit range of TR gas is roughly 6–40%. The larger the SOC of the battery, the higher the risk of explosion. In comparing several common types of batteries, the thermal safety performance of LFP is the best but it also has the disadvantages of low energy density and poor electrical conductivity.

To prevent TR cells from spreading within the module and thus causing major fire and explosion accidents, people try to set up fire separation within the battery module. Effective fire separation can block the TR heat and flame, extend the TR propagation time, avoid the occurrence of large-area TR in the battery pack, and reduce the risk of secondary ignition of LIBs. Placing insulation and heat-absorbing materials between cells is a commonly used fire-separation measure. Expansion materials, fiberglass, aerogels, and PCMs are some of the commonly used materials, but each has different severity of defects. Currently, CPCMs seem to be the most desirable materials for thermal insulation and fire retardation. Future research could be more targeted to address the issues arising from the application of organic PCMs and IPCMs.

In conclusion, the following aspects could be taken into consideration during further research.

First, current experimental studies on the TR of LIBs and their gas-production-related characteristics are mostly conducted on fresh batteries and few experiments are considered using aged batteries. The TR characteristics and related safety performance of aged LIBs differ significantly from those of new batteries. Exploring the countermeasures and management methods for TR of LIBs requires an extensive comprehension and exploration of the mechanisms of battery aging. The species and volume fraction of TR gas are the basis for conducting gas hazards and other related studies. Various factors affect the gas species and volume fraction. The current research on the influence of each element is relatively simple and the influence mechanism should be further explored, especially the impact of battery aging on TR gas production.

Second, research on the toxicity of TR gas mainly focuses on common toxic gases, such as CO and HF. The results obtained from GC-MS analysis demonstrate that more than 100 distinct species of organic compounds were detected during combustion [91]. These organic products from combustion (COPs) have been identified as potent irritants to the

human skin, eyes, and nasal passages. Therefore, organic toxic gases, such as toluene, should also be considered.

Third, the evaluation indicators are relatively single in gas explosion risk evaluation, usually only considering the two parameters of explosion limit and explosion overpressure. Also, the flame propagation speed and temperature of flame propagation, the temperature of smoke, etc., should be considered.

Finally, a more in-depth study on the mechanism and heat generation process of battery TR is needed to apply CPCM to battery thermal management and TR mimicry. More practical battery experiments and theoretical calculations should be taken to examine the feasibility of CPCM extension.

**Author Contributions:** Conceptualization, M.Q. and B.C.; methodology, J.L. and Y.C.; writing—original draft preparation, M.Q.; writing—review and editing, J.L. and B.C.; visualization M.Q. and Y.C.; supervision, J.L.; funding acquisition, J.L. All authors have read and agreed to the published version of the manuscript.

**Funding:** This research was funded by the Science and Technology Commission of Shanghai Municipality, grant number 22dz1201100.

**Data Availability Statement:** Data sharing not applicable.

**Conflicts of Interest:** The authors declare no conflict of interest. The funders had no role in the design of the study; in the collection, analyses, or interpretation of data; in the writing of the manuscript; or in the decision to publish the results.

## References

- Wang, Q.; Mao, B.; Stolarov, S.I.; Sun, J. A review of lithium ion battery failure mechanisms and fire prevention strategies. *Prog. Energy Combust. Sci.* **2019**, *73*, 95–131. [[CrossRef](#)]
- Huang, L.; Liu, L.; Lu, L.; Feng, X.; Han, X.; Li, W.; Zhang, M.; Li, D.; Liu, X.; Sauer, D.U.; et al. A review of the internal short circuit mechanism in lithium-ion batteries: Inducement, detection and prevention. *Int. J. Energy Res.* **2021**, *45*, 15797–15831. [[CrossRef](#)]
- Liao, Z.; Zhang, S.; Li, K.; Zhang, G.; Habetler, T.G. A survey of methods for monitoring and detecting thermal runaway of lithium-ion batteries. *J. Power Sources* **2019**, *436*, 226879. [[CrossRef](#)]
- Mallick, S.; Gayen, D. Thermal behaviour and thermal runaway propagation in lithium-ion battery systems A critical review. *J. Energy Storage* **2023**, *62*, 106894. [[CrossRef](#)]
- Tran, M.-K.; Mevawalla, A.; Aziz, A.; Panchal, S.; Xie, Y.; Fowler, M. A Review of Lithium-Ion Battery Thermal Runaway Modeling and Diagnosis Approaches. *Processes* **2022**, *10*, 1192. [[CrossRef](#)]
- Zhang, J.; Zhang, L.; Sun, F.; Wang, Z. An Overview on Thermal Safety Issues of Lithium-ion Batteries for Electric Vehicle Application. *IEEE Access* **2018**, *6*, 23848–23863. [[CrossRef](#)]
- Cui, Y.; Liu, J. Research progress of water mist fire extinguishing technology and its application in battery fires. *Process Saf. Environ. Prot.* **2021**, *149*, 559–574. [[CrossRef](#)]
- Chen, C.; Liu, J.; Xing, X.; Wang, Z.; Zheng, J. Review of Research on Flue Gas Components Produced by Thermal Runaway of Lithium-ion Batteries. *Mod. Chem. Res.* **2021**, *20*–21.
- Cui, X.; Cong, X.; Zhao, L. Research progress in thermalrunaway gases and explosion hazards of Li-ion battery. *Battery Bimon.* **2021**, *51*, 407–411.
- Li, H.; Tang, X.; Shao, D.; Liang, J. Research progress in thermal runaway gas of Li-ion battery. *Battery Bimon.* **2023**, *53*, 98–102. [[CrossRef](#)]
- Ren, D.; Feng, X.; Han, X.; Lu, L.; Ouyang, M. Recent Progress on Evolution of Safety Performance of Lithium-ion Battery during Aging Process. *Energy Storage Sci. Technol.* **2018**, *7*, 10. [[CrossRef](#)]
- Wang, Q.; Ping, P.; Zhao, X.; Chu, G.; Sun, J.; Chen, C. Thermal runaway caused fire and explosion of lithium ion battery. *J. Power Sources* **2012**, *208*, 210–224. [[CrossRef](#)]
- Ouyang, D.; Chen, M.; Huang, Q.; Weng, J.; Wang, Z.; Wang, J. A Review on the Thermal Hazards of the Lithium-Ion Battery and the Corresponding Countermeasures. *Appl. Sci.* **2019**, *9*, 2483. [[CrossRef](#)]
- Liu, B.; Jia, Y.; Yuan, C.; Wang, L.; Gao, X.; Yin, S.; Xu, J. Safety issues and mechanisms of lithium-ion battery cell upon mechanical abusive loading: A review. *Energy Storage Mater.* **2020**, *24*, 85–112. [[CrossRef](#)]
- Jia, Y.; Uddin, M.; Li, Y.; Xu, J. Thermal runaway propagation behavior within 18650 lithium-ion battery packs: A modeling study. *J. Energy Storage* **2020**, *31*, 101668. [[CrossRef](#)]
- Sharma, N.; Peterson, V.K. Overcharging a lithium-ion battery: Effect on the LixC 6 negative electrode determined by in situ neutron diffraction. *J. Power Sources* **2013**, *244*, 695–701. [[CrossRef](#)]

17. Yi, L.; Xu, H. Research in light transmission characteristics of 1-dimensional photonic crystal. *Opt.-Int. J. Light Electron Opt.* **2012**, *123*, 314–318. [[CrossRef](#)]
18. Wang, H.; Liu, J.; Gu, Z.; Zhu, Y.; Fu, Y.; Tao, Z.; Zhang, Q. Analysis of the thermal stability of a battery under overcharge and over-discharge. *J. Phys. Conf. Ser.* **2021**, *2009*, 12022. [[CrossRef](#)]
19. Wang, Q.; Huang, P.; Ping, P.; Du, Y.; Li, K.; Sun, J. Combustion behavior of lithium iron phosphate battery induced by external heat radiation. *J. Loss Prev. Process Ind.* **2017**, *49*, 961–969. [[CrossRef](#)]
20. Peng, P.; Jiang, F. Thermal safety of lithium-ion batteries with various cathode materials: A numerical study. *Int. J. Heat Mass Transf.* **2016**, *103*, 1008–1016. [[CrossRef](#)]
21. Yi, W.; Saurabh, S.; Yinjiao, X.; Youren, W.; Chuan, L.; Winco, Y.; Michael, P. Analysis of Manufacturing-Induced Defects and Structural Deformations in Lithium-Ion Batteries Using Computed Tomography. *Energies* **2018**, *11*, 925.
22. Röder, P.; Stiaszny, B.; Ziegler, J.C.; Baba, N.; Lagaly, P.; Wiemhöfer, H.-D. The impact of calendar aging on the thermal stability of a  $\text{LiMn}_2\text{O}_4$ - $\text{Li}(\text{Ni}_{1/3}\text{Mn}_{1/3}\text{Co}_{1/3})\text{O}_2$ /graphite lithium-ion cell. *J. Power Sources* **2014**, *268*, 315–325. [[CrossRef](#)]
23. Han, X.; Ouyang, M.; Lu, L.; Li, J.; Zheng, Y.; Li, Z. A comparative study of commercial lithium ion battery cycle life in electrical vehicle: Aging mechanism identification. *J. Power Sources* **2014**, *251*, 38–54. [[CrossRef](#)]
24. Huang, H. Study on Safety of Lithium-Ion Batteries. Ph.D. Thesis, Graduate School of Chinese Academy of Sciences, Beijing, China, 2005.
25. Huang, H.; Xie, J. Over-charge performances of lithium ion batteries after different cycles. *Chin. J. Power Sources* **2005**, *4*–7, 633.
26. Zhang, L. Study on Influencing Factors of Safety for Lithium Battery. Master’s Thesis, Yanshan University, Qinghuangdao, China, 2012.
27. Xu, Z.; Li, X.; Jia, L.; Chen, B.; Dai, Z.; Zheng, L. Effect of overcharge cycle on capacity attenuation and safety of lithium-ion batteries. *Energy Storage Sci. Technol.* **2022**, *11*, 3978–3986.
28. Friesen, A.; Horsthemke, F.; Monnighoff, X.; Brunklaus, G.; Krafft, R.; Borner, M.; Risthaus, T.; Winter, M.; Schappacher, F.M. Impact of cycling at low temperatures on the safety behavior of 18650-type lithium ion cells: Combined study of mechanical and thermal abuse testing accompanied by post-mortem analysis. *J. Power Sources* **2016**, *334*, 1–11. [[CrossRef](#)]
29. Zhang, Q.; Qu, Y. Research on the Toxicity of Gases of Thermal Runaway Released from Ternary Lithium-ion Batteries Featuring Cyclic Aging Process. *J. Beijing Univ. Aeronaut. Astronaut.* **2022**, *1*–10.
30. Larsson, F.; Bertilsson, S.; Furlani, M.; Albinsson, I.; Mellander, B.-E. Gas explosions and thermal runaways during external heating abuse of commercial lithium-ion graphite- $\text{LiCoO}_2$  cells at different levels of ageing. *J. Power Sources* **2018**, *373*, 220–231. [[CrossRef](#)]
31. Boerner, M.; Friesen, A.; Gruetzke, M.; Stenzel, Y.P.; Brunklaus, G.; Haetge, J.; Nowak, S.; Schappacher, F.M.; Winter, M. Correlation of aging and thermal stability of commercial 18650-type lithium ion batteries. *J. Power Sources* **2017**, *342*, 382–392. [[CrossRef](#)]
32. Xie, S.; Ren, L.; Yang, X.; Wang, H.; Sun, Q.; Chen, X.; He, Y. Influence of cycling aging and ambient pressure on the thermal safety features of lithium-ion battery. *J. Power Sources* **2020**, *448*, 227425. [[CrossRef](#)]
33. Zhang, J.; Su, L.; Li, Z.; Sun, Y.; Wu, N. The Evolution of Lithium-Ion Cell Thermal Safety with Aging Examined in a Battery Testing Calorimeter. *Batteries* **2016**, *2*, 12. [[CrossRef](#)]
34. Chen, D.; Hao, C.; Liu, T.; Han, Z.; Zhang, W. Raman Spectrum Analysis Method of Thermal Runaway Gas from Lithium-ion Batteries. *Zhongguo Jiguang/Chin. J. Lasers* **2022**, *49*, 2311001. [[CrossRef](#)]
35. Feng, X.; Ouyang, M.; Liu, X.; Lu, L.; Xia, Y.; He, X. Thermal runaway mechanism of lithium ion battery for electric vehicles: A review. *Energy Storage Mater.* **2018**, *10*, 246–267. [[CrossRef](#)]
36. Guo, C.; Zhao, H. Study on thermal runaway gas release characteristics of lithium-ion battery under different state of charge. *Technol. Innov. Appl.* **2020**, *28*–31.
37. Somandepalli, V.; Marr, K.; Horn, Q. Quantification of Combustion Hazards of Thermal Runaway Failures in Lithium-Ion Batteries. *SAE Int. J. Altern. Powertrains* **2014**, *3*, 98–104. [[CrossRef](#)]
38. Golubkov, A.W.; Scheikl, S.; Planteu, R.; Voitic, G.; Wiltsche, H.; Stangl, C.; Fauler, G.; Thaler, A.; Hacker, V. Thermal runaway of commercial 18650 Li-ion batteries with LFP and NCA cathodes—Impact of state of charge and overcharge. *RSC Adv.* **2015**, *5*, 57171–57186. [[CrossRef](#)]
39. Ribière, P.; Grugeon, S.; Morcrette, M.; Boyanov, S.; Laruelle, S.; Marlar, G. Investigation on the fire-induced hazards of Li-ion battery cells by fire calorimetry. *Energy Environ. Sci.* **2012**, *5*, 5271–5280. [[CrossRef](#)]
40. Golubkov, A.W.; Fuchs, D.; Wagner, J.; Wiltsche, H.; Stangl, C.; Fauler, G.; Voitic, G.; Thaler, A.; Hacker, V. Thermal-runaway experiments on consumer Li-ion batteries with metal-oxide and olivine-type cathodes. *RSC Adv.* **2014**, *4*, 3633–3642. [[CrossRef](#)]
41. Koch, S.; Fill, A.; Birke, K.P. Comprehensive gas analysis on large scale automotive lithium-ion cells in thermal runaway. *J. Power Sources* **2018**, *398*, 106–112. [[CrossRef](#)]
42. Huang, Z.; Li, X.; Wang, Q.; Duan, Q.; Li, Y.; Li, L.; Wang, Q. Experimental investigation on thermal runaway propagation of large format lithium ion battery modules with two cathodes. *Int. J. Heat Mass Transf.* **2021**, *172*, 121077. [[CrossRef](#)]
43. Fleischhammer, M.; Waldmann, T.; Bisle, G.; Hogg, B.-I.; Wohlfahrt-Mehrens, M. Interaction of cyclic ageing at high-rate and low temperatures and safety in lithium-ion batteries. *J. Power Sources* **2015**, *274*, 432–439. [[CrossRef](#)]
44. Chen, F. Study on the Heat Generation Characteristics of High-Specific-Energy Lithium Ion Batteries with NCA Cathode during Aging. Ph.D. Thesis, Zhejiang University, Hangzhou, China, 2021.

45. Sun, J.; Li, J.; Dang, S.; Tang, N.; Zhou, T.; Li, J.; Wei, S.; Yang, K.; Fei, G. Research of toxic productions from thermal runaway processes of Li-ion battery and materials. *Energy Storage Sci. Technol.* **2015**, *4*, 7. [[CrossRef](#)]
46. Larsson, F.; Andersson, P.; Blomqvist, P.; Lorén, A.; Mellander, B.-E. Characteristics of lithium-ion batteries during fire tests. *J. Power Sources* **2014**, *271*, 414–420. [[CrossRef](#)]
47. Larsson, F.; Andersson, P.; Blomqvist, P.; Mellander, B.E. Toxic fluoride gas emissions from lithium-ion battery fires. *Sci. Rep.* **2017**, *7*, 10018. [[CrossRef](#)] [[PubMed](#)]
48. Gueguen, A.; Streich, D.; He, M.; Mendez, M.; Chesneau, F.F.; Novak, P.; Berg, E.J. Decomposition of LiPF<sub>6</sub> in high energy lithium-ion batteries studied with online electrochemical mass spectrometry. *J. Electrochem. Soc.* **2016**, *163*, A1095–A1100. [[CrossRef](#)]
49. Lecocq, A.; Eshetu, G.G.; Grugeon, S.; Martin, N.; Laruelle, S.; Marlair, G. Scenario-based prediction of Li-ion batteries fire-induced toxicity. *J. Power Sources* **2016**, *316*, 197–206. [[CrossRef](#)]
50. Yuan, S.; Chang, C.; Yan, S.; Zhou, P.; Qian, X.; Yuan, M.; Liu, K. A review of fire-extinguishing agent on suppressing lithium-ion batteries fire. *J. Energy Chem.* **2021**, *62*, 262–280. [[CrossRef](#)]
51. Zhang, L.; Duan, Q.; Meng, X.; Jin, K.; Xu, J.; Sun, J.; Wang, Q. Experimental investigation on intermittent spray cooling and toxic hazards of lithium-ion battery thermal runaway. *Energy Convers. Manag.* **2022**, *252*, 115091. [[CrossRef](#)]
52. ISO 13571; Life-Threatening Components of Fire-Guidelines for the Estimation of Time to Compromised Tenability in Fires. ISO: Geneva, Switzerland, 2012.
53. Tong, Z.; Yin, Y.; Huang, Q.; Lin, F. Review on quantitative evaluation methods of fire smoke toxicity. *J. Saf. Environ.* **2005**, *05*, 101–105.
54. Zhang, Q.; Qu, Y.; Liu, T. A methodology study on risk analysis for thermal runaway gas toxicity of lithium batteries. *J. Beijing Univ. Aeronaut. Astronaut.* **2022**, *1*–10.
55. Peng, Y.; Yang, L.; Ju, X.; Liao, B.; Ye, K.; Li, L.; Cao, B.; Ni, Y. A comprehensive investigation on the thermal and toxic hazards of large format lithium-ion batteries with LiFePO<sub>4</sub> cathode. *J. Hazard Mater.* **2020**, *381*, 120916. [[CrossRef](#)]
56. Cui, Y.; Liu, J.; Cong, B.; Han, X.; Yin, S. Characterization and assessment of fire evolution process of electric vehicles placed in parallel. *Process Saf. Environ. Prot.* **2022**, *166*, 524–534. [[CrossRef](#)]
57. Cui, Y.; Cong, B.; Liu, J.; Qiu, M.; Han, X. Characteristics and Hazards of Plug-In Hybrid Electric Vehicle Fires Caused by Lithium-Ion Battery Packs with Thermal Runaway. *Front. Energy Res.* **2022**, *10*, 878035. [[CrossRef](#)]
58. Lamb, J.; Orendorff, C.J.; Roth, E.P.; Langendorf, J. Studies on the thermal breakdown of common Li-ion battery electrolyte components. *J. Electrochem. Soc.* **2015**, *162*, A2131–A2135. [[CrossRef](#)]
59. Tian, G.; Yu, C.; Li, X. Study on Calculation Method of Gas Explosion Limits. *Gas Heat* **2006**, *29*–33. [[CrossRef](#)]
60. Li, W.; Wang, H.; Zhang, Y.; Ouyang, M. Flammability characteristics of the battery vent gas: A case of NCA and LFP lithium-ion batteries during external heating abuse. *J. Energy Storage* **2019**, *24*, 100775. [[CrossRef](#)]
61. Guo, C.; Zhang, Q. Determination on explosion limit of pyrolysis gas released by lithium-ion battery and its risk analysis. *J. Saf. Sci. Technol.* **2016**, *12*, 4.
62. Zhang, Q.; Niu, J.; Zhao, Z.; Wang, Q. Research on the effect of thermal runaway gas components and explosion limits of lithium-ion batteries under different charge states. *J. Energy Storage* **2022**, *45*, 103759. [[CrossRef](#)]
63. Karp, M.E. Flammability Limits of Lithium-Ion Battery Thermal Runaway Vent Gas in Air and the Inerting Effects of Halon 1301. Master’s Thesis, Graduate School-New Brunswick, New Brunswick, NJ, USA, 2016. [[CrossRef](#)]
64. Chen, S.; Wang, Z.; Wang, J.; Tong, X.; Yan, W. Lower explosion limit of the vented gases from Li-ion batteries thermal runaway in high temperature condition. *J. Loss Prev. Process Ind.* **2019**, *63*, 103992. [[CrossRef](#)]
65. Ma, B.; Liu, J.; Yu, R. Study on the Flammability Limits of Lithium-Ion Battery Vent Gas under Different Initial Conditions. *ACS Omega* **2020**, *5*, 28096–28107. [[CrossRef](#)]
66. Baird, A.R.; Archibald, E.J.; Marr, K.C.; Ezekoye, O.A. Explosion hazards from lithium-ion battery vent gas. *J. Power Sources* **2020**, *446*, 227257. [[CrossRef](#)]
67. Niu, Z.; Jiang, X.; Xie, B.; Jin, Y. Study on Simulation and Safety Protection of Electric Vehicle Overcharge and Explosion Accident. *Diangong Jishu Xuebao/Trans. China Electrotech. Soc.* **2022**, *37*, 36–47, 57. [[CrossRef](#)]
68. Kan, Q.; Chen, M.; Ren, C. Experimental study on thermal runaway gas explosion characteristics of lithium ion battery. *Fire Sci. Technol.* **2021**, *40*, 959–962.
69. Cui, Y.; Liu, J.; Han, X.; Sun, S.; Cong, B. Full-scale experimental study on suppressing lithium-ion battery pack fires from electric vehicles. *Fire Saf. J.* **2022**, *129*, 103562. [[CrossRef](#)]
70. Liu, Z. Research on Thermal Management System of Power Battery Coupled with Composite Phase Change Material and Liquid Cooling. Ph.D. Thesis, Nanchang University, Nanchang, China, 2022.
71. Zhang, W.; Liang, Z.; Yin, X.; Ling, G. Avoiding thermal runaway propagation of lithium-ion battery modules by using hybrid phase change material and liquid cooling. *Appl. Therm. Eng.* **2021**, *184*, 116380. [[CrossRef](#)]
72. Berdichevsky, E.M.; Cole, P.D.; Hebert, A.J.; Hermann, W.A.; Kelty, K.R.; Kohn, S.I.; Lyons, D.F.; Straubel, J.B.; Mendez, N.J. Mitigation of Propagation of Thermal Runaway in a Multi-Cell Battery Pack. U.S. Patent 7433794, 7 October 2008.
73. Mehta, V.H.; Prilutsky, A.; Hermann, W.A. Cell Thermal Runaway Propagation Resistance Using an Internal Layer of Intumescence Material. U.S. Patent 20100075221, 24 August 2010.

74. Lopez, C.F.; Jeevarajan, J.A.; Mukherjee, P.P. Experimental analysis of thermal runaway and propagation in lithium-ion battery modules. *J. Electrochem. Soc.* **2015**, *162*, A1905–A1915. [[CrossRef](#)]
75. Chen, C.; Niu, H.; Li, Z.; Li, L.; Mo, S.; Huang, X. Thermal Runaway Propagation Mitigation of Lithium Ion Battery by Epoxy Resin Board. *Energy Storage Sci. Technol.* **2019**, *8*, 532–537.
76. Qin, S. Experimental Study on Thermal Runaway of Potassium Lithium-ion Battery Based on Packaging Materials. *Technol. Innov. Appl.* **2017**, *180*–181.
77. Chang, R. Study on Thermal Runaway Propagation Prevention of lithium-Ion Battery Based on Thermal Insulation Layer. Master’s Thesis, Shandong University of Technology, Zibo, China, 2022.
78. Zhang, Z.; Yang, X.; Xu, C.; Wang, M. Research Progress of Aerogel Insulation Materials for Lithium-ion Power Batteries. *China Build. Mater. Sci. Technol.* **2023**, *32*, 62–68.
79. Hu, Q. Study on Lithium-Ion Batteries Thermal Runaway Propagation Characteristics and Blocking Techniques. Master’s Thesis, China Ship Scientific Research Center, Wuxi, China, 2015.
80. Shen, X.D.; Duan, Q.; Qin, P.; Wang, Q.; Sun, J. Experimental study on thermal runaway mitigation and heat transfer characteristics of ternary lithium-ion batteries. *Energy Storage Sci. Technol.* **2023**, *12*, 1862–1871. [[CrossRef](#)]
81. Ping, P.; Dai, X.; Kong, D.; Zhang, Y.; Zhao, H.; Gao, X.; Gao, W. Experimental study on nano-encapsulated inorganic phase change material for lithium-ion battery thermal management and thermal runaway suppression. *Chem. Eng. J.* **2023**, *463*, 142401. [[CrossRef](#)]
82. Wilke, S.; Schweitzer, B.; Khateeb, S.; Al-Hallaj, S. Preventing thermal runaway propagation in lithium ion battery packs using a phase change composite material: An experimental study. *J. Power Sources* **2017**, *340*, 51–59. [[CrossRef](#)]
83. Zhi, W.; Jian, W. Investigation of external heating-induced failure propagation behaviors in large-size cell modules with different phase change materials. *Energy* **2020**, *204*, 117946. [[CrossRef](#)]
84. Weng, J.; Xiao, C.; Ouyang, D.; Yang, X.; Chen, M.; Zhang, G.; Yuen, R.K.K.; Wang, J. Mitigation effects on thermal runaway propagation of structure-enhanced phase change material modules with flame retardant additives. *Energy* **2022**, *239*, 122087. [[CrossRef](#)]
85. Dai, X.; Kong, D.; Du, J.; Zhang, Y.; Ping, P. Investigation on effect of phase change material on the thermal runaway of lithium-ion battery and exploration of flame retardancy improvement. *Process Saf. Environ. Prot.* **2022**, *159*, 232–242. [[CrossRef](#)]
86. Talele, V.; Patil, M.S.; Panchal, S.; Fraser, R.; Fowler, M. Battery thermal runaway propagation time delay strategy using phase change material integrated with pyro block lining: Dual functionality battery thermal design. *J. Energy Storage* **2023**, *65*, 107253. [[CrossRef](#)]
87. Weng, J.; Ouyang, D.; Yang, X.; Chen, M.; Zhang, G.; Wang, J. Alleviation of thermal runaway propagation in thermal management modules using aerogel felt coupled with flame-retarded phase change material. *Energy Convers. Manag.* **2019**, *200*, 112071. [[CrossRef](#)]
88. Zhou, Z.; Zhou, X.; Li, M.; Cao, B.; Liew, K.M.; Yang, L. Experimentally exploring prevention of thermal runaway propagation of large-format prismatic lithium-ion battery module. *Appl. Energy* **2022**, *327*, 120119. [[CrossRef](#)]
89. Galazutdinova, Y.; Ushak, S.; Farid, M.; Al-Hallaj, S.; Grageda, M. Development of the inorganic composite phase change materials for passive thermal management of Li-ion batteries: Application. *J. Power Sources* **2021**, *491*, 229624. [[CrossRef](#)]
90. Cao, J.; Ling, Z.; Lin, S.; He, Y.; Fang, X.; Zhang, Z. Thermochemical heat storage system for preventing battery thermal runaway propagation using sodium acetate trihydrate/expanded graphite. *Chem. Eng. J.* **2022**, *433*, 133536. [[CrossRef](#)]
91. Sun, J.; Li, J.; Zhou, T.; Yang, K.; Wei, S.; Tang, N.; Dang, N.; Li, H.; Qiu, X.; Chen, L. Toxicity, a serious concern of thermal runaway from commercial Li-ion battery. *Nano Energy* **2016**, *27*, 313–319. [[CrossRef](#)]

**Disclaimer/Publisher’s Note:** The statements, opinions and data contained in all publications are solely those of the individual author(s) and contributor(s) and not of MDPI and/or the editor(s). MDPI and/or the editor(s) disclaim responsibility for any injury to people or property resulting from any ideas, methods, instructions or products referred to in the content.